CHAPTER 7

IN VIVO STUDIES

7.1 Introduction

Nanoparticles offer a way to improve the nose-to-brain drug delivery since they are able to protect the encapsulated drug from biological and/or chemical degradation, and extracellular transport by P-gp efflux proteins. This would increase CNS availability of the drug. A high relative surface area means that these vectors will release drug faster than larger equivalents. Their small diameter potentially allows nanoparticles to be transported transcellularly through olfactory neurones to the brain via the various endocytic pathways of sustentacular or neuronal cells in the olfactory membrane. Additionally, surface modification of the nanoparticles could further aid in achieving targeted CNS delivery of a number of different drugs using the same 'platform' delivery system which has known and well characterised biophysical properties and mechanism(s) of transit into the CNS.

However, the effectiveness of nose to brain delivery can be ascertained only through in vivo studies. These studies can either be pharmacodynamic or pharmacokinetic. One of the major advantages of nose to brain delivery is the improvement in bioavailability of drugs in the brain. It effectively aids in surpassing the Blood Brain Barrier, and targets the drug to the different sites of brain (Mistry, Stolnik, & Illum, 2009).

Bioavailability is one of the principal pharmacokinetic properties of drugs. It is one of the essential tools in pharmacokinetics, as bioavailability must be considered when calculating dosages for non-intravenous routes of administration. It is a subcategory of absorption and is the fraction of an administered dose of unchanged drug that reaches the systemic circulation. Relative bioavailability or bioequivalence is the most common measure for comparing the bioavailability of one formulation of the same drug to another. The mean responses such as C_{max} and AUC are compared to determine relative bioavailability. The AUC refers to the extent of bioavailability while C_{max} refers to the rate of bioavailability.

7.2 Animals

Male Sprague - Dawley rats weighing 200-250 g were used for in vivo studies for both Galantamine nanoparticles and Bapineuzumab nanoparticles. Animals were housed in propylene cages (38cm×23cm×10cm) under laboratory conditions of controlled environment of temperature 30±2 ◦C and 60±5% RH. Three rats per cage were fed ad libitum with animal feed allowing free access to drinking water. The rats were acclimatized in a 12h light/12h dark constant temperature for one week prior to experiments. All surgical and experimental procedures for pharmacokinetic studies involving Galantamine were reviewed and approved by the Animal Ethics Committee of Institute of Pharmaceutical Education and Research, Wardha, Maharashtra. The experimental procedures for in vivo study involving Bapineuzumab were approved by the Animal Ethics Committee of Department of Pharmacy, M S University of Baroda, Vadodara. All animal experiments were approved by Committee for the Purpose of Control and Supervision of Experiments on Animals (CPCSEA), Ministry of Social Justice and Empowerment, Government of India, New Delhi, India.

7.3 *In vivo* Pharmacokinetics Studies for Galantamine hydrobromide loaded Nanoparticles

7.3.1 Methods

Animals were divided into 2 groups. Each group contained 6 rats. One group received drug solution in saline via i.v.(intravenous) route and other group received the Galantamine hydrobromide loaded nanoparticulate formulation via intranasal route. The doses for both the groups were 1.75 mg/kg of Galantamine (Leonard et al., 2005). The intra venous animal group was administered 100 µL of Galantamine hydrobromide solution (sterile) through the tail vein in bolus. Prior to nasal administration to the second group, the rats were anaesthetized by intramuscular administration of Ketamine (100 mg/kg). 50 µL of lyophilized nanoparticle formulation suspended in distilled water were administered in each nostril using a polyurethane tube ((24G X19 mm)

attached to a microliter syringe. The tube was inserted about 10 mm deep into one of the nares, enabling the delivery of the formulation towards the roof of the nasal cavity. During this administration, the rats were kept in slanted position of approximate 15º to the perpendicular for 3 – 5 seconds to prevent the formulation to drain from the nasal cavity and entry into the esophageal passage (Serralheiro, Alves, Fortuna, & Falcao, 2014).

0.5 mL of blood sample were taken from the retrorbital plexus at each time point of 0.5, 1, 2, 3, 4, 5 and 6 hour respectively. The rats in the intranasal group were anaesthetized by intraperitoneal administration of Ketamine (5 mg/kg). The CSF (0.5 mL) were collected by means of a puncture using a 25 mm gauge 5 mm polyethylene tube at time points 0.5, 1, 2, 3, 4, 5 and 6 hour respectively.

For Cerebrospinal fluid withdrawal, rat was anaesthetised using ketamine (5mg/kg). Rat was mounted on stereotaxic apparatus (M. C. Dalal agencies, Chennai) using earbars. Fur (Hairs) on dorsal part of rat head was cut using scissors and incision was made between eyes part (vertically at centre). Skin was retracted using artery forcep to right and left side and skull was exposed to make sutures visible (Skin part was rubbed using cotton plug).

Following the procedure of Paxinos and Watson (1986) (*The Mouse Brain in Stereotaxic Coordinates*, 1997) bregma was located.

Using the dental driller, burr hole was made in skull without damaging the brain (to avoid perfused bleeding) using the co-ordinates: 1.33 mm right lateral, 0.8mm posterior and 1.5 mm ventral). Polyethylene tubing was inserted in hole and cerebrospinal fluid was suctioned out and collected for analysis of drug in it. Incision was surgically ligated using sutures and antibiotics were applied for a week topically (Neosporin,) and intramuscularly (tetracycline, 10 mg/kg).

The withdrawn samples were processed and analyzed by HPLC as described in the analytical methods chapter (Chapter no.3).

7.3.2 Results and discussions

The plasma drug concentration versus time profile for plain drug solution administered intravenously and Galantamine hydrobromide loaded nanoparticles after nasal delivery in rats (n=6) at drug concentration of 1.75 mg/kg (Leonard et al., 2005) are shown in Figure 8.1. Table 8.1 gives the plasma concentrations of Galantamine hydrobromide after intravenous administration and after intranasal administration of nanoparticles at different time points. The pharmacokinetic parameters including C_{max} (in µg/ml) and T_{max} – the maximum drug concentration encountered after the drug administration and the time at which C_{max} is reached AUC_{0-inf} (ng h/ml) – the total area under the curve which represents the *in vivo* therapeutic effects, $t_{1/2}$ (h) – the half-life of the drug in the plasma and relative bioavailability were analysed using PK Solver (Y. Zhang, Huo, Zhou, & Xie, 2010).

Table 7.1: Concentration of Galantamine hydrobromide in plasma after intra venous drug solution and intranasal nanoparticle administration.

Time (hours)	**Galantamine hydrobromide solution (µg/mL)***	**Galantamine hydrobromide nanoparticles. (µg/mL)***
0.5	7.13±0.58	4.6±1.39
1	5.02±1.28	0.983±0.214
2	2.23±0.87	0.975±0.56
3	1.78±0.58	0.88±0.19
4	1.5±0.47	1.42±0.31
5	1.32±0.25	0.702±0.66
6	1.28±0.38	0.512±0.31

*: Standard deviation from 6 animals

The non compartmental analyses are shown in Table 8.2. After intravenous administration, the C_{max} of 7.13 µg/mL was achieved. After intranasal administration, the formulation demonstrated systemic absorption with a C_{max} of about 4.6 µg/mL.

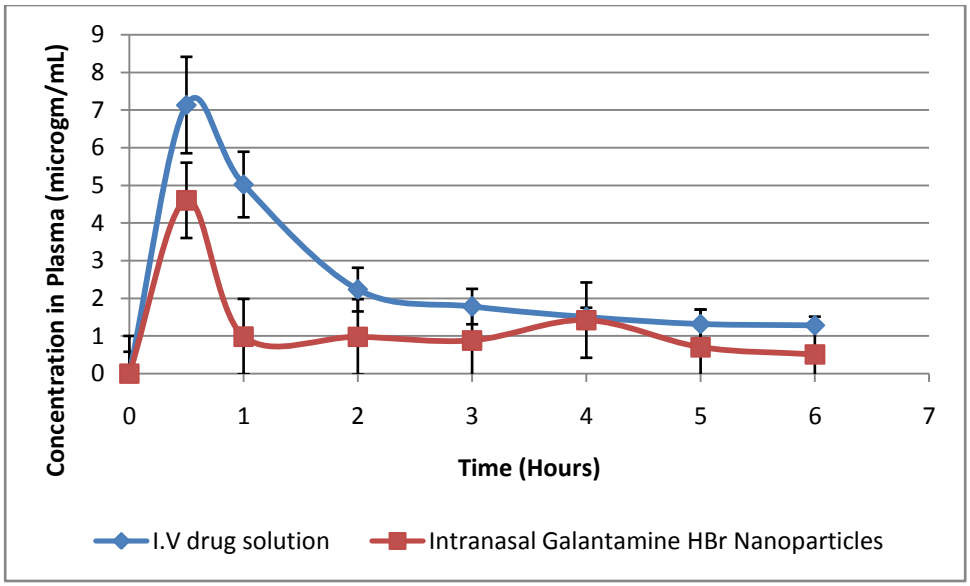

Figure 7.1: Plasma concentration versus time profile for Galantamine hydrobromide after intra venous drug solution and intranasal nanoparticle administration.

From Figure 7.1, it can be seen that following intravenous administration, the absolute bioavailability of Galantamine Hydrobromide in plasma was much higher than what was observed after intranasal administration.

Table 7.2: Pharmacokinetic parameters with respect to plasma for Galantamine hydrobromide after intra venous drug solution and intranasal nanoparticle administration.

	C_{max} (µg/mL)	**T_{max} (hour)**	**AUC $_{0-t}$ (µg/mL*h)**	**AUC $_{0-\infty}$ (µg/mL*h)**	**$T_{1/2}$ (hour)**	**MRT (hour)**
Plain drug solution (i.v)	7.13±0.58	0.5±0.06	17.55±2.10	26.63±3.19	4.92±0.59	5.66±0.97
Nanoparticles (i.n)	4.6±1.39	0.5±0.13	7.27±1.81	8.29±2.07	1.35±0.34	3.04±0.76

Data represented as mean ± S.D (n = 6)

Table 7.2 represents the pharmacokinetic data with respect to plasma after intravenous administration of Galantamine hydrobromide drug solution and intranasal

Galantamine hydrobromide nanoparticle formulation. For both the solution and the nanoparticles, the T_{max} was achieved in 0.5 hour indicating rapid systemic absorption of Galantamine hydrobromide after intranasal administration. However, the C_{max} was higher after intravenous administration than intranasal formulation. This was a general observation as the drug directly enters into plasma. The C_{max} and AUC for intranasal administration were lower than for intravenous drug solution pointing towards other biodistribution pathways. Intranasal administration was expected to provide CNS targeting, which would reduce its plasma levels (Colombo et al., 2011).

The dose for both the routes were same, hence the clear difference in bioavailability. While drug bioavailability is complete with i.v. injection, this is not the case with all other administration routes (Colombo et al., 2011).

Table 7.3: Concentration of Galantamine hydrobromide in Cerebrospinal fluid after intra venous drug solution and intranasal nanoparticle administration.

Time (hours)	**Galantamine hydrobromide solution (µg/mL) (i.v)***	**Galantamine hydrobromide nanoparticles. (µg/mL)(i.n)***
0.5	0.31 ± 0.15	0.82 ± 0.11
1	0.57 ± 0.11	1.11 ± 0.16
2	0.82 ± 0.10	1.27 ± 0.22
3	0.44 ± 0.08	1.48 ± 0.17
4	0.29 ± 0.07	0.85 ± 0.18
5	0.21 ± 0.05	0.55 ± 0.20
6	0.18 ± 0.09	0.33 ± 0.15

*: Standard deviation from 6 animals

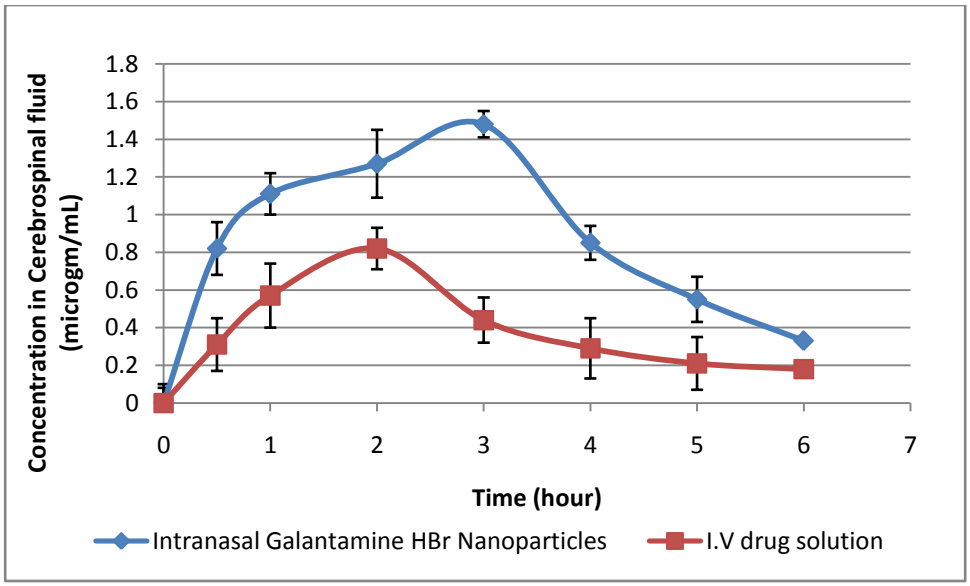

Figure 7.2: Cerebrospinal fluid concentration versus time profile for Galantamine hydrobromide after intra venous drug solution and intranasal nanoparticle administration.

Table 7.4: Pharmacokinetic parameters for cerebrospinal fluid of Galantamine hydrobromide after intra venous drug solution and intranasal nanoparticle administration.

	C_{max} (µg/mL)	T_{max} (hour)	AUC $_{0-t}$ (µg/mL*h)	AUC $_{0-\infty}$ (µg/mL*h)	$T_{1/2}$ (hour)	MRT (hour)
Plain drug solution (i.v)	0.82 ± 0.07	2.00 ± 0.94	2.44 ± 0.85	3.06 ± 0.99	2.35 ± 0.79	3.19 ± 0.63
Nanoparticles (i.n)	1.58 ± 0.21	3.00 ± 0.14	5.62 ± 1.22	6.28 ± 1.47	1.42 ± 0.33	3.31 ± 0.51

Figure 7.2 clearly shows that the cerebrospinal fluid concentration of Galantamine hydrobromide after nasal administration was higher than what was achieved after intravenous administration, suggesting its entry in to the brain via the olfactory neurons. It is also important to note that the drug although in lower concentration was detected in Cerebrospinal fluid after intravenous administration. As Galantamine hydrobromide is highly hydrophilic, an active transport mechanism could justify its presence in the CNS following i.v. injection (Colombo et al., 2011).

From Table 7.4 it could be seen that, C_{max} for plain drug solution was only 0.82 µg/ml, due to the inability to effectively pass the blood brain barrier. C_{max} for the nanoparticles was found to be 1.58 µg/ml, which was significantly higher than the plain drug solution ($p < 0.01$). A higher C_{max} for nanoparticles was achieved as it could directly enter the brain through the olfactory neuron, thereby surpassing the Blood Brain Barrier. This was possible due to its smaller size and hence improved surface characteristics.

The $AUC_{0-\infty}$ for plain drug solution was 3.06 µg/mL*h whereas for nanoparticles it was 6.28 µg/mL*h. Hence there was a twofold improvement in CNS bioavailability of Galantamine hydrobromide after nasal delivery ($p < 0.01$). This could be attributed to various transport mechanisms that are widely reported for direct nose to brain delivery (Illum, 2003; Wang, Jiang, & Lu, 2003). For a hydrophilic drug like Galantamine hydrobromide, a paracellular pathway is more likely, which is more aqueous in nature.

To further understand the targeting of Galantamine hydrobromide to the brain, two parameters viz: Drug Targeting Index and Direct Brain Transport Percent were calculated (Q. Zhang et al., 2004).

The Drug Targeting Index was calculated using the formula:

$$DTI = (AUC_{CSF} / AUC_{Plasma})_{i.n.} / (AUC_{CSF} / AUC_{Plasma})_{i.v.} \quad \text{.....(8.1)}$$

The Direct Brain Transport Percentage was calculated using the formula:

$$DTP\ (\%) = [(B_{i.n.} - B_x / B_{i.n}]\ \text{x } 100 \text{.....(8.2)}$$

The Drug Targeting Index was found to be 6.91 whereas the direct brain transport percentage was found to be 84.87%. It is assumed that if drug concentration in the brain is significantly higher after intranasal administration , or DTI >1, a direct pathway from the nasal olfactory region to the brain exists. The higher the DTI is, the better the drug targeting to brain can be expected after i.n. administration (Mittal et al., 2014).

These values further support the existence of alternate routes through the nose to deliver the drug to brain via the olfactory pathways.

7.4 *In vivo* study for passive immunization with Bapineuzumab nanoparticles

7.4.1 Method

(1) Surgical procedure:(Liu et al., 2013)

Aβ $_{25–35}$ (Sigma Aldrich, India) was dissolved in saline (5 mg/ml) and was incubated for 7 days at 37 ◦C, while ibotenic acid (Sigma Aldrich, India) was dissolved in PBS (10 mg/ml). Before surgery, four aliquots of Aβ $_{25–35}$ solution and one aliquot of IBO solution were mixed to a final concentration of Aβ $_{25–35}$ at 4 mg/ml and Ibotenic acid at 2 mg/ml. The rats were anaesthetized with ketamine (Qualigens, India) following i.p. injection (5 mg/kg), and then placed in a stereotaxic instrument. 2.5 µl of the mixture solution of Aβ $_{25–35}$ and ibotenic acid was subsequently injected over 5 min through a Hamilton syringe into rat bilateral hippocampus (3.5 mm posterior to the bregma, ±2.0 mm lateral to the midline and 2.7 mm ventral from the skull surface). After injection, the needle was left in place for additional 5 min before withdrawal. Sham-operated animals were injected with the same volume of saline.

(2) Drug administration and treatment: (Liu et al., 2013)

One week after co-injection of Aβ 25–35 and Ibotenic acid, the rats were distributed into four groups of three each. The first group was sham wherein the rats had been surgically injected only saline instead of amyloid inducing agent. The Alzheimer's disease control group received only saline intranasally after surgery to induce amyloid plaques. The third group received intranasal nanoparticle formulation. The fourth group received intravenous solution of Bapineuzumab. The doses for both the routes were same (2 mg/kg). Sham control group received intranasal administration of saline. The treatment in all the groups was continued for fourteen days.

(3) Preparation of samples: (Liu et al., 2013)

After, the rats were euthanized with an overdose of pentobarbital (100 mg/kg), an incision was made in the skin over the skull of rats. Then the skull was cut

open and the intact brain was carefully removed from the skull. The brain was quickly rinsed with normal saline and wiped with Kimberly-Clarks wipes to remove the blood. It was cut into two part dorsally and the hippocampal region was removed. After collection of brain tissue it was immediately stored at −40 ◦C until analysis. Prior to analysis, the samples were allowed to thaw. Then the weight was noted, and homogenized using a tissue homogenizer. It was then suspended in Phosphate Buffer Saline and centrifuged at 2000 rpm. The supernatant was analyzed for amyloid content.

(4) Analysis of amyloid activity by Enzyme Linked Immunosorbent Assay:

The analysis of amyloid reduction after administration of intranasal nanoparticles or intravenous solution was conducted using ELISA. For this, the standard kit (SunRed Bio, China) was utilized and the protocol mentioned therein was followed. The kit utilized double – antibody sandwich enzyme – linked immunosorbent assay to assay the level of human amyloid beta peptide 1-42 in samples. The procedure was similar to what was followed in Chapter 5. A standard calibration was plotted through a range of concentration from 50-400 ng/mL of human amyloid beta peptide 1-42 and the samples were analyzed against standard calibration curve. For calibration, standard amyloid solution provided in the kit was diluted using the diluent solution provided in the kit. The microtitre plate was read photometrically at 450 nm in a microplate reader (BioRad, India).

7.4.2 Results and discussions

The standard calibration curve for ELISA is shown in Figure 7.3.

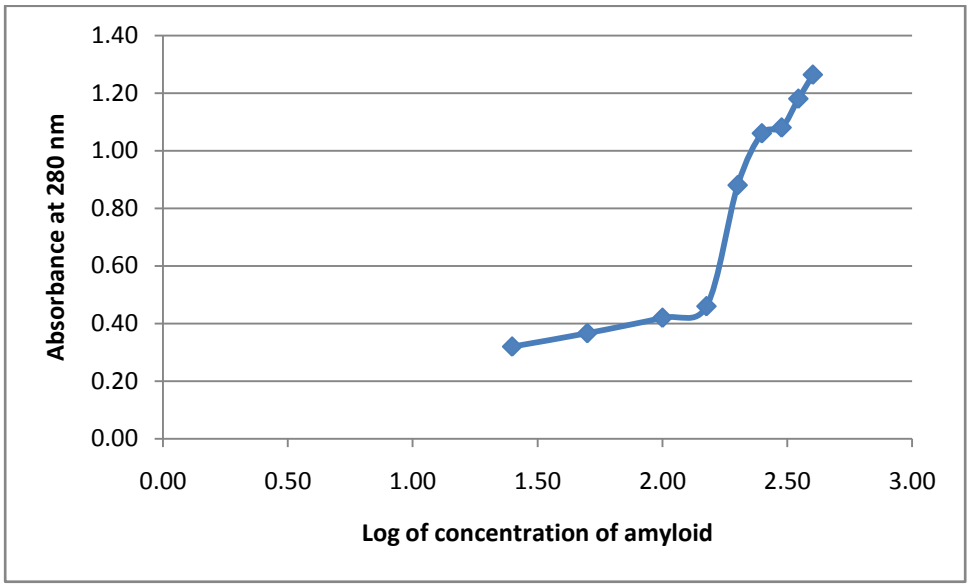

Figure 7.3: Standard calibration curve for amyloid concentration.

The reduction of amyloid concentration was calculated on the 1st, 7th, and 14th day of the studies.

Figure 7.4 shows the reduction in amyloid concentration after intranasal administration of nanoparticles with respect to the sham group. The result is shown for the reduction on 1st, 7th, and 14th day of the treatment. The amyloid reduction was the maximum on the 14th day, thereby showing the effect of Bapineuzumab in reducing the amyloid load .

Table 7.5: Concentration of amyloid after intranasal administration of antibody nanoparticles.

	0 day (i.v)	7 days (i.v)	14 days (i.v)	Sham control	AD control
Average concentration (ng/mL)*	56.67±1.52	75.67±2.08	97 ± 2.64	23.67 ± 1.53	262.33 ± 10.97

*: Studies were carried out in triplicate

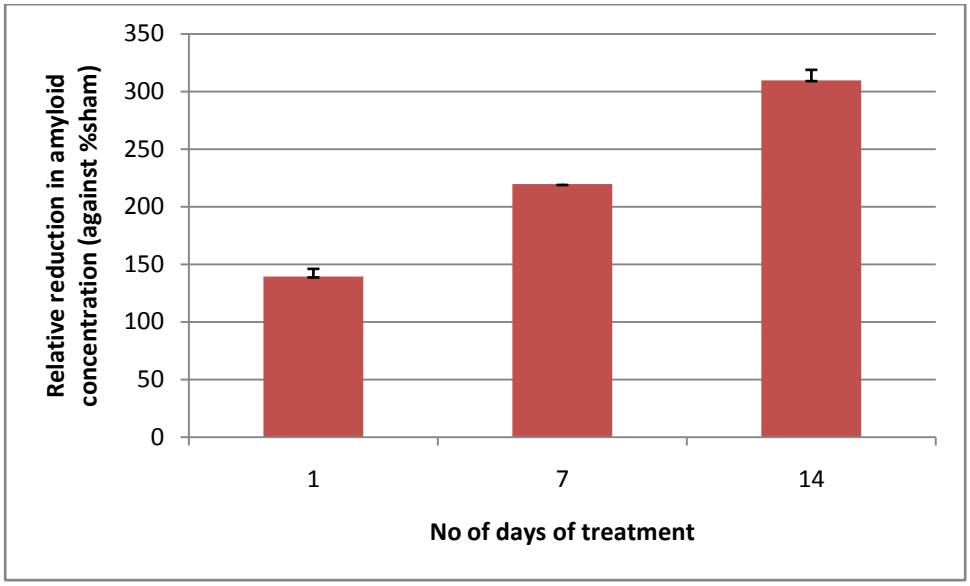

Figure 7.4: Relative reduction in amyloid concentration after intranasal administration of nanoparticles.

Table 7.6: Concentration of amyloid after intravenous administration of antibody solution.

	0 day (i.v)	7 days (i.v)	14 days (i.v)	Sham control	AD control
Average concentration (ng/mL)*	123.33± 12.91	150 ±11.18	185.66 ±20.84	23.67±1.53	262.33 ± 10.97

*: Studies were carried out in triplicate.

Figure 7.5 shows the reduction in amyloid concentration after intravenous administration of antibody solution with respect to the sham group. The result is

shown for the reduction on 1st, 7th, and 14th day of the treatment. The amyloid reduction is the maximum on the 14th day.

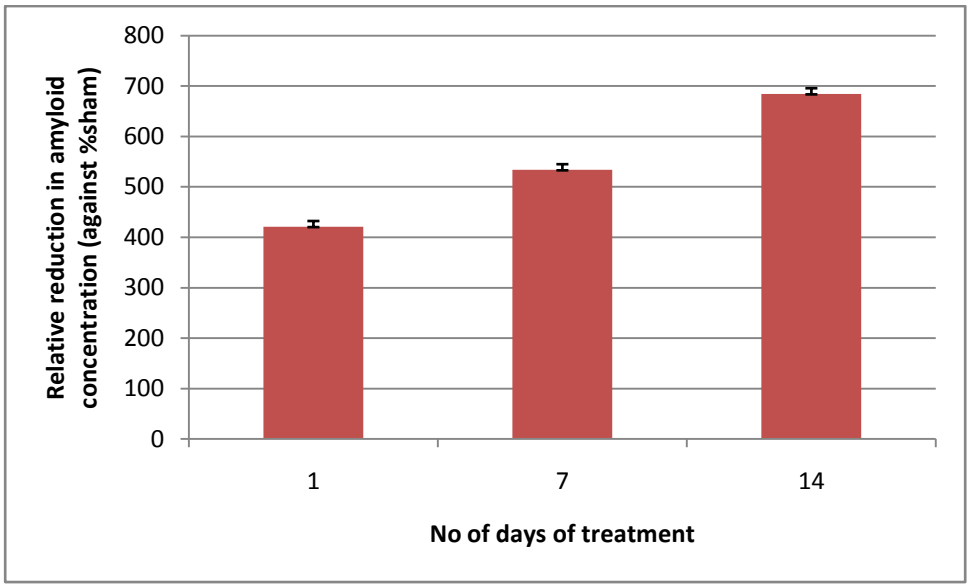

Figure 7.5: Relative reduction in amyloid concentration after intravenous administration of antibody solution.

On comparing both the data, it could be seen that intranasal nanoparticles reduced the amyloid load significantly ($p < 0.01$) in comparison to intravenous administration. The data recorded for intranasal administration was significantly higher ($p < 0.01$) than what was achieved for intravenous administration. From Figure 7.4, the amyloid reduction after intra nasal administration relative to sham control group was 139 % on the first day which progressively increased to 219 % on the 7th day and, 309.85% on the 14th day. This indicated towards Bapineuzumab's ability to deplete amyloid from the affected site in the brain. The antibody being an anti amyloid antibody, it's repeated administration increased the antibody generation in the animals leading to decreased amyloid load. This mechanism forms the basis of passive immunization. Additonally, the active immunization techniques and its effect on amyloid deposition can be mimicked by passive administration of anti – amyloid antibodies(Bard et al., 2000) .

Therefore, nasal administration of Bapineuzumab loaded nanopaticles open up possibilities of passive immunization, by promising delivery of the antibody to the actual target that is brain.

7.5 References

- Bard, F., Cannon, C., Barbour, R., Burke, R. L., Games, D., Grajeda, H., . . . Yednock, T. (2000). Peripherally administered antibodies against amyloid beta-peptide enter the central nervous system and reduce pathology in a mouse model of Alzheimer disease. *Nat Med, 6*(8), 916-919. doi: 10.1038/78682
- Colombo, G., Lorenzini, L., Zironi, E., Galligioni, V., Sonvico, F., Balducci, A. G., . . . Scagliarini, A. (2011). Brain distribution of ribavirin after intranasal administration. *Antiviral Res, 92*(3), 408-414. doi: 10.1016/j.antiviral.2011.09.012
- Illum, L. (2003). Nasal drug delivery--possibilities, problems and solutions. *J Control Release, 87*(1-3), 187-198.
- Leonard, A. K., Sileno, A. P., MacEvilly, C., Foerder, C. A., Quay, S. C., & Costantino, H. R. (2005). Development of a novel high-concentration galantamine formulation suitable for intranasal delivery. *J Pharm Sci, 94*(8), 1736-1746. doi: 10.1002/jps.20389
- Liu, Z., Jiang, M., Kang, T., Miao, D., Gu, G., Song, Q., . . . Chen, J. (2013). Lactoferrin-modified PEG-co-PCL nanoparticles for enhanced brain delivery of NAP peptide following intranasal administration. *Biomaterials, 34*(15), 3870-3881. doi: 10.1016/j.biomaterials.2013.02.003
- Mistry, A., Stolnik, S., & Illum, L. (2009). Nanoparticles for direct nose-to-brain delivery of drugs. *International Journal of Pharmaceutics, 379*(1), 146-157. doi: http://dx.doi.org/10.1016/j.ijpharm.2009.06.019
- Mittal, D., Ali, A., Md, S., Baboota, S., Sahni, J. K., & Ali, J. (2014). Insights into direct nose to brain delivery: current status and future perspective. *Drug Deliv, 21*(2), 75-86. doi: 10.3109/10717544.2013.838713
- *The Mouse Brain in Stereotaxic Coordinates*. (1997). San Diego: Academic Press.
- Serralheiro, A., Alves, G., Fortuna, A., & Falcao, A. (2014). Intranasal administration of carbamazepine to mice: a direct delivery pathway for brain targeting. *Eur J Pharm Sci, 60*, 32-39. doi: 10.1016/j.ejps.2014.04.019
- Wang, F., Jiang, X., & Lu, W. (2003). Profiles of methotrexate in blood and CSF following intranasal and intravenous administration to rats. *Int J Pharm, 263*(1-2), 1-7.
- Zhang, Q., Jiang, X., Jiang, W., Lu, W., Su, L., & Shi, Z. (2004). Preparation of nimodipine-loaded microemulsion for intranasal delivery and evaluation on the targeting efficiency to the brain. *Int J Pharm, 275*(1-2), 85-96. doi: 10.1016/j.ijpharm.2004.01.039
- Zhang, Y., Huo, M., Zhou, J., & Xie, S. (2010). PKSolver: An add-in program for pharmacokinetic and pharmacodynamic data analysis in Microsoft Excel. *Comput Methods Programs Biomed, 99*(3), 306-314. doi: 10.1016/j.cmpb.2010.01.007